

Controlled nanostructures at $\text{La}_{0.7}\text{Sr}_{0.3}\text{MnO}_3$ thin film surfaces formed by STM lithography

LIU, Yun

*Department of Physics,
Norwegian University of Science and Technology,
Trondheim 7491, Norway*

ZHANG, Jia

*School of Mechanical Engineering,
University of South China,
Hengyang, 421001, China*

Abstract

Nanoscale lithography on $\text{La}_{0.7}\text{Sr}_{0.3}\text{MnO}_3$ (LSMO) thin film surfaces has been performed by scanning tunneling microscopy under ambient conditions. From line-etching experiments we found that the line depth is increasing in a step-wise fashion with increasing bias voltage as well as with decreasing scan speed. On average, the depth of the etched lines is an integral multiple of the LSMO out-of-plane lattice constant about 0.4 nm. A minimum wall thickness of 1.5 nm was obtained between etched lines. We have utilized the ability to control the etched line depths to create complicated inverse-pyramid nanostructure. Our work shows the feasibility of using STM lithography to create controllable and complex nanoscale structures in LSMO thin film.

Keyword: Scanning tunneling microscopy; $\text{La}_{0.7}\text{Sr}_{0.3}\text{MnO}_3$; Thin film; Lithography

PACS numbers:

I. INTRODUCTION

Perovskite manganites with chemical formula $\text{La}_{1-x}\text{A}_x\text{MnO}_3$ (where $\text{A} = \text{Sr}, \text{Ba}, \text{Ca}$ or Pb) have attracted large scientific interests due to their abundant but complex physical properties, such as colossal magnetoresistance (CMR)^{1,2}, metal-insulator transition^{3,4}, spin-, charge-, and orbital-ordering^{5,6} as well as phase coexistence^{7,8,9}. Some of the physical properties have been proved to be strongly dependent on material dimension down to nanometer length scale, for example, Takamura et al¹⁰ found that magnetic domain structures in $\text{La}_{0.7}\text{Sr}_{0.3}\text{MnO}_3$ (LSMO) thin films could be controlled by varying shape (square, diamond, and circular) and size (diameters ranging from ~ 140 nm to $1\mu\text{m}$) of patterned islands. Therefore exploring those properties especially at the nanoscale length plays a critical role in the study of manganites. Moreover, owing to their CMR effect and high Curie temperature, the new generation of spintronic devices is expected to exploit perovskite manganites as major components. In particular, LSMO is showing a Curie temperature as high as 370 K at intermediate hole doping¹¹, and could serve as an promising candidate for room temperature sensor and memory applications. Consequently finding proper ways to create nanoscale structures on perovskite manganite thin film surfaces are crucial not only for understanding of basic phenomena at the nanoscale level but also for fabrication of spintronic devices.

Scanning probe microscopy (SPM) based lithography¹² has been a prevailing tool for controlled patterning on different materials at the sub-100 nm length scale following the pioneering work done by Dagata et al in 1990¹³. Since then, this technique has been successfully used to fabricate nanostructures on graphite^{14,15}, metals (Au ^{16,17,18}, Ti ¹⁹, Al ²⁰, and Cr ²¹), semiconductors (Si ^{22,23}, SiO_2/Si ²⁴, and GaAs ²⁵) and perovskite oxides ($\text{YBa}_2\text{Cu}_3\text{O}_7$ ^{26,27,28}, SrTiO_3 ^{29,30}, SrRuO_3 ³² and $\text{La}_{0.8}\text{Ba}_{0.2}\text{MnO}_3$ ^{30,31}), etc. In general, the surface modification has been found to be strongly dependent on etching parameters such as bias voltage, tunneling current, scan speed, scan repetitions and ambient. For instance, constant threshold voltage was observed for hole formation on gold above a critical relative humidity¹⁸ as well as for surface modification on graphite surface covered with water¹⁵, whereas the threshold voltage was found to be dependant on the tunneling current for the

hole formation on silicon²³. In line etching experiments on SrRuO₃ thin film surfaces, the depth of etched lines was observed to increase with increasing bias voltage and scan repetitions, while it decreased with increasing scan speed³². Li et al^{30,31} conducted atomic force microscope (AFM) lithography on La_{0.8}Ba_{0.2}MnO₃ films using conductive tips (Si cantilever coated by Pt, Cr-Co and W₂C) in contact mode. They found that only operation of negative sample bias voltage created patterns with excellent controllability and reproducibility. They also found that the pattern height increased with increasing sample bias at first, then stabilized at different fixed voltages. The smallest pattern width and interval were measured to be ~ 50 nm by Pt or W₂C coated tips. The etching mechanisms in SPM lithography are complicated and still under discussion. Among others, widely proposed mechanisms are chemical reactions^{14,17,27}, field evaporation^{22,23,26,27,28}, local heating³³, electromigration³⁴, and combinations of these.

In the present work, we have exploited the feasibility of using scanning tunneling microscope (STM) to create controlled nanoscale structures at LSMO thin film surfaces. The influence of different etching parameters has been addressed through line etching experiments. The minimum wall thickness between etched lines has been determined. Furthermore, we have successfully created complicated nanostructures resembling inverse pyramid. Most importantly, this work shows that nanostructures can be etched by STM in LSMO in a highly controlled manner.

II. EXPERIMENTAL

LSMO thin films were deposited on TiO₂ terminated, single crystal SrTiO₃ substrates by pulsed laser deposition (from TSST) using a 248 nm KrF excimer laser in an oxygen atmosphere with pressure 0.2 mBar. The laser energy is 50 mJ per pulse. The substrate temperature was 850°C during deposition. In situ RHEED monitoring of the growth showed a continuous growth rate of 60 Å/min. Films at thickness 120 nm were used for the etching experiments. Structure and surface characterization were performed using a high resolution x-ray diffractometer (Bruker AXS D8) and an AFM (Digital Instruments Nanoscope III), respectively.

The nanoscale lithography experiments were conducted in air at room tempera-

ture with the AFM system operated in STM mode. Both Platinum/Iridium (Pt/Ir) and pure iridium (Ir) tips were used. Images of the etched patterns were recorded in situ after the lithographic process with the same tips. Both imaging and lithography were performed in constant current mode. Tunneling parameters for STM imaging both before and after the etching process were a positive tip (negative sample) bias voltage of 500 mV and a tunneling current of 500 pA. The same tunneling parameters combined with sharp step edges seen in the STM images were used as an indication of similar tip quality before and after etching. During the lithographic process, the tip movement was defined by a NanoscriptTM programme. All the etching experiments were conducted at large positive tip bias voltages (≥ 2.8 V). An ac current component with frequency 50Hz and amplitude 40-60 pA was imposed to 60 pA setpoint tunneling current during STM lithography to prevent material build-up during etching³². In addition, by adjusting the integral and proportional gains in the feedback loop, the vertical oscillation amplitude of the STM tip could be controlled within 1 nm. This method not only improved the quality of the lithographic structures but also hindered possible damage to the The tip by material build-up on the surface.

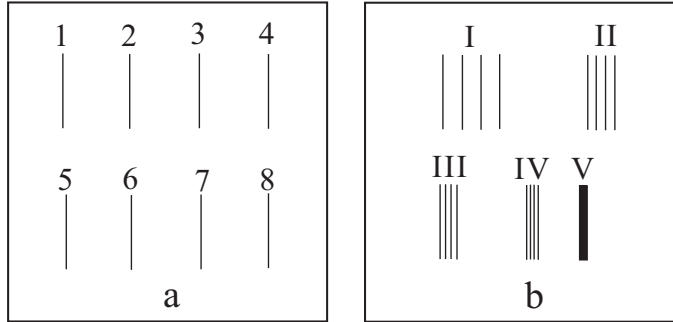


FIG. 1: Schematics of (a) eight-line pattern and (b) pattern for wall thickness determination.

Figure 1(a) illustrates the eight-line pattern etched during the line-etching experiments. The eight-line patterns were created using bias voltages ranging from 2.8 V to 3.6 V, a tunneling current of 60 pA, scan speeds from 500 nm/s to 1500 nm/s and 100 scan repetitions per line. The length of each etched line was 100 nm. The upper left line was etched first and the lower right last, the sequence is indicated by

the numbers in figure 1(a). Figure 1(b) shows the patterns etched to determine the thicknesses of walls formed between etched lines. The etching parameters are bias voltages of 3.2 V, 3.4 V and 3.6 V, a tunneling current of 60 pA, scan speeds of 500 nm/s and 1000 nm/s, and 100 scan repetitions per line. From these experiments a minimum wall thickness was determined below which areas could be formed by numerous line etchings. Schematic three-step process of creating inverse-pyramid structures is shown in 2. First, the largest square was etched on the LSMO surface (left panel), then the second largest square was created inside the largest one (middle panel), and finally the smallest one likewise (right panel). The same etching parameters were used through all three steps. Bias voltages of 3.2 V and 3.4 V were selected to create inverse-pyramid structure while other parameters were fixed at scan speed 1000 nm/s, tunneling current 60 pA, and 100 scans per line.

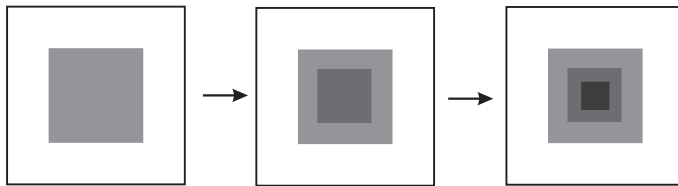


FIG. 2: Schematics representation of etching procedures for (a) inverse-pyramid and (b) pyramid nanostructure formation.

III. RESULTS AND DISCUSSION

From the x-ray diffraction measurements we determined the out of plane c parameter of the LSMO films to be ~ 3.85 Å, calculated from the (001), (002) and (003) diffraction peaks. This value is slightly lower than the bulk value of 3.88 Å, and corresponds to an in-plane tensile strain associated with epitaxial growth on the larger unit cell of SrTiO_3 . The surface of the films displayed the step-and-terrace topography, with atomically flat plateaus, separated by steps of integral unit cell step heights. The RMS roughness was measured to be approximately 0.14 nm. Four point RT measurements showed metallic behavior (at room temperature $R = 5 \times 10^{-3} \text{ Ohm} \cdot \text{cm}$).

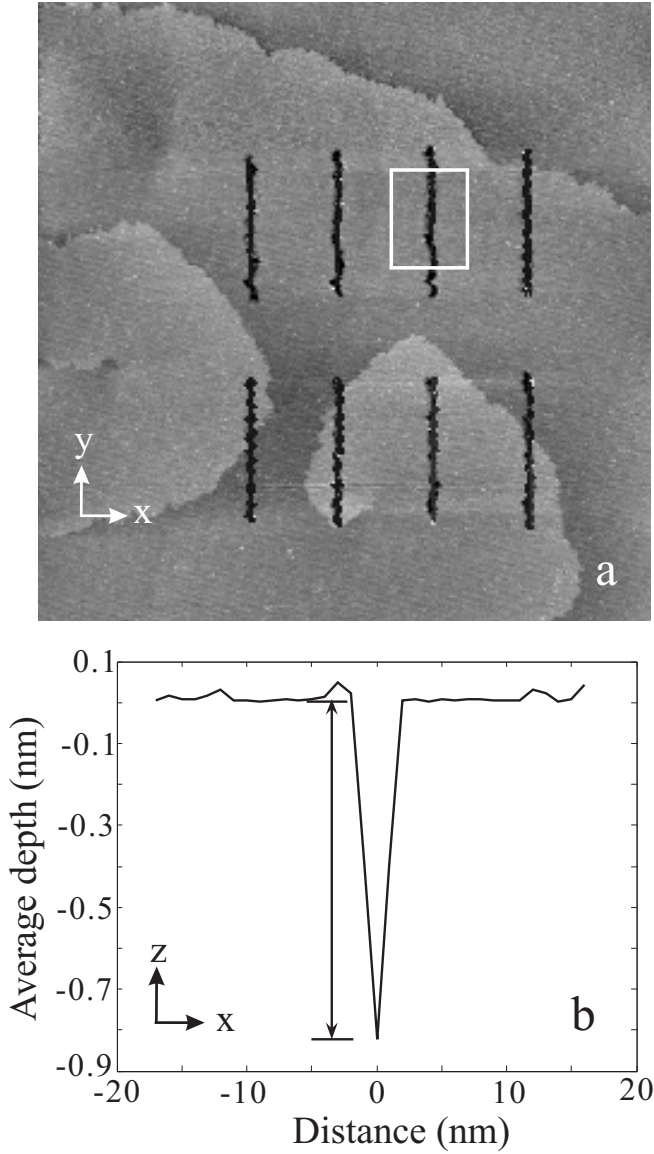


FIG. 3: (a) STM image ($500\text{nm} \times 500\text{nm}$) of eight etched lines from the line etching experiments. Each line was 100nm long and etched at bias voltage 3.4V , tunneling current 60pA , scan speed 1000nm/s and 100 scan repetitions per line. (b) section profile from the area confined by the dashed-line box. Each data point represents the average depths measured along the y -direction inside the marked area for each x -position.

Figure 3(a) shows an STM image of an eight-line pattern etched at a bias voltage of 3.4 V , scan speed 1000 nm/s , tunneling current 60pA and 100 scans per line. The depth profile across an etched line is displayed in 3(b). The average depth at

each x-position is determined from the depths measured along the y-direction inside the marked area with length 70 nm along y. The two end parts of each line were removed in the depth determination because there is a time lag when the tip is changing direction at the ends of each line, leading to deeper etching. Additionally, we define a line to be successfully etched when the surface modification is continuous for at least 70 nm with a minimum average depth of half a unit cell, that is 0.2 nm. Only successful lines were analyzed.

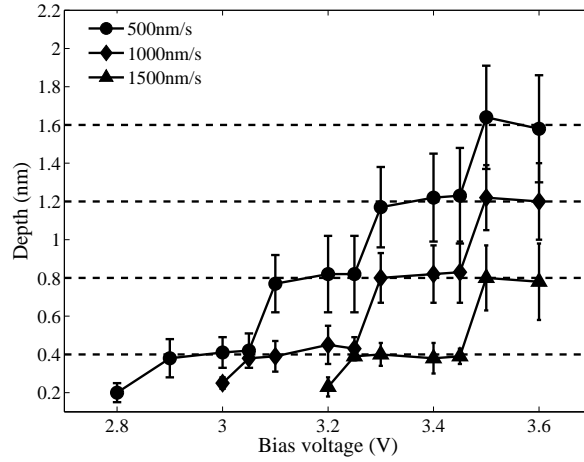


FIG. 4: Dependence of etched line depth on bias voltage and scanspeed. The scan repetition for each line is 100 and the setpoint tunneling current is 60 pA. 40 lines were calculated for each set of voltage and scan speed. The error bars are standard deviation and the solid lines are guides to the eye.

The depth determined from the line etching experiments are summarized in figure 4. We plot the line depth as a function of bias voltage using 100 scan repetitions per line for scan speeds of 500, 1000 and 1500 nm/s. Generally, the line depth increases with increasing bias voltage in a stepwise fashion with a step size of about 0.4 nm. Inversely, the depth increases with decreasing scan speed. It should be mentioned that there are three data points around 0.2 nm with very short errorbars. This is partly a consequence of the chosen definition of successful etching. As is evident from comparing the etching results at the three different scan speeds, the longer line etching time corresponds to slower scan speed. This finding is supported by another set of experiments (not shown) revealing that a larger number of scan repetitions

per line leads to larger line depth. Thus, the STM lithography is a time dependent process. These results are in agreement with earlier studies of STM etching of SrRuO_3 ³², where also the line depth was found to increase with the numbers of scan repetitions per line as well as decreasing scan speed.

The most significant observation in figure 4 is the change in the average line depth in steps of ~ 0.4 nm, that is, the average line depths are distributed around four levels: 0.4 nm, 0.8 nm, 1.2 nm and 1.6 nm, which are integral multiples of the out-of-plane lattice constant (~ 0.4 nm) of the LSMO unit cell. To our knowledge, this is the first work by STM lithography to manipulate material surfaces at step of unit cell. The only exception from this behavior is the observed etching close to threshold where a depth of 0.2 nm corresponding to half a unit cell is obtained. The reason for the sub unit cell etching at the outermost surface region of LSMO thin films may be related to the broken symmetry at the surface. However, we could not observe half unit cell steps on the LSMO thin films surfaces. The etching results at bias voltages of 3.05 V, 3.25 V and 3.45 V indicate that there are critical bias voltages at which a transition between different etching depths occurs. These findings suggest that it is possible to control the depth of etched structure in LSMO with unit cell precision.

At a given scan speed, we could identify threshold voltages below which no etching occurs. For STM etching on SrRuO_3 ³², it is also found that the threshold voltage depends on scan speed. In AFM lithography on LBMO films using Pt-coated tip, at scan speed of 500 nm/s, Li et al³¹ reported a threshold voltage of ~ 3 V at positive tip bias, which is very similar to our results showing a threshold voltage of 2.8 V at the same scan speed. They also observed that the depth of the pattern was found to increase with increasing bias voltage linearly at first, but to saturate at ~ 8 nm where the bias voltage reached ~ 7 V. Bias voltages up to 12 V were applied. In our experiment, the line depth increases in a stepwise manner with increasing bias voltage, and the tip quality strongly influence the etching results. At bias voltages above 3.6 V, mounds or debris were formed on the surfaces and multi-tips were created during etching, indicating that the Pt/Ir tip deteriorated above 3.6 V. This large different in upper limit for the applied voltage can be explained by the sharper tips applied in the present work. Sharper tips result in a stronger electric

field formed between the tip and the sample at lower voltages as compared blunter AFM tips. At negative tip bias voltages, we observed both mounds and etched lines appeared alternatively on LSMO surface, indicating the evaporation from both tip and sample.

The different line depth values obtained in the line etching experiments suggest that controlled etching by STM can be performed in LSMO thin film surfaces. To determine the minimum wall thickness which can be obtained between two consecutive etched lines, tests of 4-line patterns with decreasing separation were performed. Figure 5(a) shows five sets of etched lines with different wall thicknesses. Figure 5(b) is a plot of wall thickness against programmed line separation. The offset between programmed line separation and wall thickness is ~ 0.5 nm. For programmed line separations 6 nm (I), 3 nm (II) and 2 nm (III), the lines are separated by continuous walls. When the line separation is 1.5 nm (IV), the walls are not continuous. Finally at a line separation of 1 nm (V), the walls collapse, forming a homogeneous etched area. Thus the minimum line width with continuous walls from these experiments was determined to be 1.5 nm. The structures in both figure 5 (a) was etched using a bias voltage of 3.2 V, tunneling current of 60 pA, 1000 nm/s scan speed and 100 scan repetitions per line. Most SPM-based lithography techniques are able to create patterns with spatial resolution on the order of 10 nm¹². In their experiments performing AFM lithography on LBMO thin films, Li et al³¹ reported both the line width and intervals are less than 50 nm. For other established techniques, such as photolithography³⁵, the minimum feature size is 30 nm, for focus ion beam milling, 30 nm and for electron beam lithography^{37,38}, 10 nm.

To demonstrate the capabilities of STM etching in LSMO we etched a nanoscale architecture: an inverse pyramid. It was constructed by combining etched lines. Figure 6 (a) shows images of the inverse pyramid. The etching parameters were the bias voltages 3.2 V, 60 pA tunneling current, 1000 nm/s scan speed and 100 scan repetitions per line were. Figure 6(b) display depth profiles along the marked lines in figure 6(a). The step heights in figure 6(a) was measured to be ~ 0.4 nm, which is consistent with the results of line etching in figure 4.

From both figure 6 (a) we observed clearly the zigzag patterns on the edges of structures. In order to investigate the influence of in-plane crystallographic

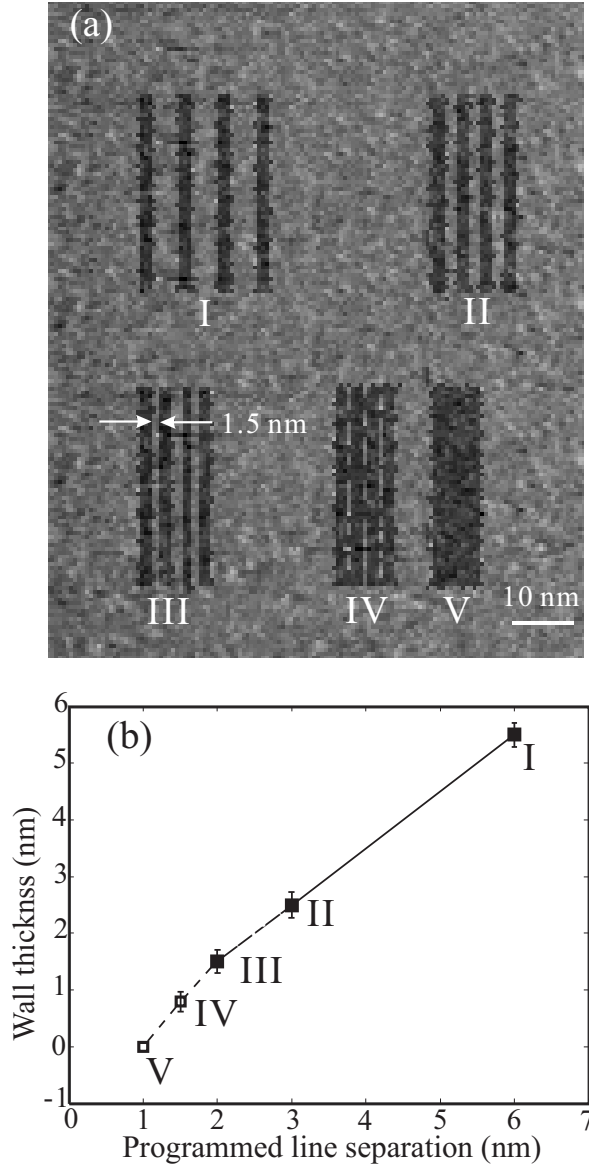


FIG. 5: (a) Wall structures with minimum sizes of 1.5 nm, as pointed out by arrows. The etching parameters were 3.2 V bias voltage, 60 pA tunneling current, 1000 nm/s scanspeed and 100 scan repetitions per line. (b) Wall thickness as a function of programmed line separation. the solid line represents continuous walls, whereas the dashed line represents non-continuous and collapsed walls.

anisotropy on this pattern, we conducted lithographic experiments through rotating sample by 0° , 45° and 90° relative to the tip scanning directions. The results indicate that there are no distinct differences in the etching results in these cases. In

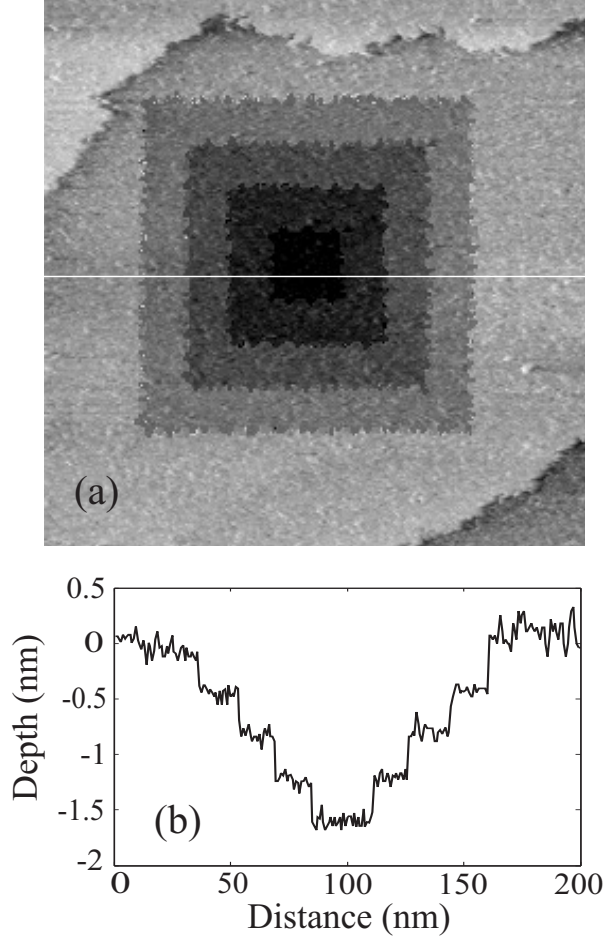


FIG. 6: (a) Inverse-pyramid structures created by applying 3.2V bias voltage with set-point tunneling current of 60pA, scanspeed of 1000nm/s and 100 scan repetitions per line. (b) Depth profiles along the mark lines in (a), showing step sizes of 0.4nm. The image area is 200nm \times 200nm

fact, the periodic interval of protrudes along both the vertical and horizontal edges is about 8 nm, hinting that this pattern could result from the interval fashion of tip movement during etching process.

IV. CONCLUSION

In summary, controlled STM lithography has been performed on perovskite manganese LSMO thin film surfaces. The line depth is found to increase with increasing

bias voltage and with decreasing scan speed at a given number of scan repetitions per line. It is observed that most values of average line depth are integral multiples of c-axis constant of LSMO unit cell. Based on line-etching experiments, we successfully created inverse-pyramid nanoscale structures. Furthermore, ~ 1.5 nm thick walls were achieved as the smallest structures from STM lithography on LSMO thin film surfaces to date.

-
- ¹ von Helmut R, Wecker J and Hopzapfel B 1993 *Phys. Rev. Lett.* **71** 2331
- ² Jin S, Tiefel T H, McCormack M, Fastnacht R A, Ramesh R and Chen L H 1994 *Science* **264** 413
- ³ Ramirez A P 1997 *J. Phys.: Condens. Matter* **9** 8171
- ⁴ Imada M, Fujimori A and Tokura Y 1998 *Rev. Mod. Phys.* **70** 1039
- ⁵ Salamon M B and Jaime M 2001 *Rev. Mod. Phys.* **73** 583
- ⁶ Coey M 2004 *Nature* **430** 155
- ⁷ Moreo A, Yunoki S and Eblio Dagotto 1999 *Science* **283** 2023
- ⁸ G. Varelogiannis 2000 *Phys. Rev. Lett.* **85** 4172
- ⁹ Dagotto E 2003 *Nanoscale Phase Separation and Collosal Magnetoresistance (Springer Series in Solid-State Sciences)* (Berlin Heidelberg: Springer)
- ¹⁰ Takamura Y, Chopdekar R V, Scholl A, Doran A, Liddle J A, Harteneck B and Suzuki Yuri 2006 *Nano Lett.* **6** 6
- ¹¹ Urushibara A, Moritomo Y, Arima T, Asamitsu A, Kido G and Tokura Y 1995 *Phys. Rev. B* **51** 14103
- ¹² Tseng A A, Notargiacomo A and Chen T P 2005 *J. Vac. Sci. Technol. B* **23** 877
- ¹³ Dagata J A, Schneir J, Harary H H, Evans C J, Postek M T and Bennett J 1990 *Appl. Phys. Lett.* **56** 2001
- ¹⁴ Albrecht T R, Dovek M M, Kirk M D, Lang C A, Quate C F and Smith D P E 1989 *Appl. Phys. Lett.* **55** 1727
- ¹⁵ Penner R M, Heben M J, lewis N S and Quate C F 1991 *Appl. Phys. Lett.* **58** 1389
- ¹⁶ Guo C X and Thomson D J 1992 *Ultramicroscopy* **42-44** 1452
- ¹⁷ Chang C S, Su W B and Tsong T T 1994 *Phys. Rev. Lett.* **72** 574
- ¹⁸ Lebreton C and Wang Z Z 1996 *J. Vac. Sci. Technol. B* **14** 1356
- ¹⁹ Irmer B, Kehrie M, Lorenz H and Kotthaus J P 1997 *Appl. Phys. Lett.* **71** 1733
- ²⁰ Snow E S, Park D and Campbell P M 1996 *Appl. Phys. Lett.* **69** 269
- ²¹ Snow E S, Campbell P M, Rendell R W, Buot F A, Park D, Marrian C R K and Magno R 2002 *Appl. Phys. Lett.* **72** 3071
- ²² Lyo I-W and Avouris P 1991 *Science* **253** 173

- ²³ Kobayashi A, Grey F, Williams R S and Aono M 1993 *Science* **259** 1724
- ²⁴ Iwasaki H, Yoshinobu T and Sudoh K 2003 *Nanotechnology* **14** R55
- ²⁵ Nagahara L A, Thundat T and Lindsay S M 1990 *Appl. Phys. Lett.* **57** 270
- ²⁶ Heyvaert I, Osquiguil E, Van Haesendonck C and Bruynseraede Y 1992 *Appl. Phys. Lett.* **61** 111
- ²⁷ Bertsche G, Clauss W, Prins F E and Kem D P 1998 *J. Vac. Sci. Technol. B* **16** 2833
- ²⁸ Fan Y C, Fitzgerald A G and Cairns J A 2000 *J. Vac. Sci. Technol. B* **18** 2377
- ²⁹ Pellegrino L, Pallecchi I, Marre D, Bellingeri E and Siri A S 2002 *Appl. Phys. Lett.* **81** 3849
- ³⁰ Li R W, Kanki T, Tanaka H, Takagi A, Matsumoto T and Kawai T 2004 *Appl. Phys. Lett.* **84** 2670
- ³¹ Li R W, Kanki T, Tohyama H-A, Hirooka M, Tanaka H and Kawai T 2005 *Nanotechnology* **16** 28
- ³² You C C, Rystad N V, Borg A and Tybell T 2007 *Appl. surf. Sci.* **253** 4704
- ³³ Li Y Z, Vazquez L, Piner R, Andres R P and Reifenberger R 1989 *Appl. Phys. Lett.* **54** 1424
- ³⁴ Eigler D M, Lutz C P and Rudge W E 1991 *Nature* **352** 600
- ³⁵ Jaeger R C 2002 *Introduction to Microelectronic Fabrication* (New Jersey: Prentice Hall)
- ³⁶ Tjerkstra R W, Segerink F B, Kelly J J and Vos W L 2008 *J. Vac. Sci. Technol. B* **26** 973
- ³⁷ Khoury M and Ferry D K 1996 *J. Vac. Sci. Technol. B* **14** 75
- ³⁸ Tseng A A, Chen K, Chen C D and Ma K J 1991 *IEEE Tran. Electron. Packag. Manuf.* **26** 141